^{35}Cl NMR studies of the domain structure of tetramethylammonium cadmium chloride (TMCC) at lower temperatures

2001 J. Phys.: Condens. Matter 13 1119

(http://iopscience.iop.org/0953-8984/13/5/325)

INSTITUTE OF PHYSICS PUBLISHING JOURNAL OF PHYSICS: CONDENSED MATTER

J. Phys.: Condens. Matter **13** (2001) 1119–1131 www.iop.org/Journals/cm PII: S0953-8984(01)19005-3

^{35}Cl NMR studies of the domain structure of tetramethylammonium cadmium chloride (TMCC) at lower temperatures

S Mulla-Osman[1], D Michel[1], G Völkel[1], I Peral[2] and G Madariaga[2]

[1] Universität Leipzig, Fakultät für Physik und Geowissenschaften, Linnéstrasse 5, D-04103 Leipzig, Germany
[2] Departamento de Física de la Materia Condensada, Facultad de Ciencias, Universidad del País Vasco, Apartado 644, 48080 Bilbao, Spain

Received 28 November 2000

Abstract

Quadrupolar perturbed ^{35}Cl NMR and ^{35}Cl NQR investigations are performed on single crystals of tetramethylammonium cadmium chloride, $(CH_3)_4NCdCl_3$ (TMCC), in order to study the formation of ferroelastic domains in the ferroelastic phase II below 118 K in which the hexagonal symmetry of the high temperature phase I is lost. The experimental results cannot simply be explained in terms of the well known monoclinic domain structure but additionally a twin domain structure is found to exist in phase II: six orientational domains are verified from the NMR rotational pattern at 113 K in contrast to the expected number of three for a classical $6/mF2/m$ transition. The rotational angle Θ between the epitaxially grown twins is calculated from the strain tensors of the three orientation states, applying an algebraic approach. The theoretical value $\Theta = 3.5^\circ$ is in very good correspondence with the experimental result from the ^{35}Cl NMR studies ($\sim 4^\circ$). Similar results were also derived in recent x-ray studies in phase II. In the low temperature phase III below 104 K the number of non-equivalent Cl positions is consistent with both the space group of phase III and the sixfold enlarged size of the unit cell in phase III with respect to that in phase I as observed in XRD studies.

1. Introduction

The crystal of TMCC, $(CH_3)_4NCdCl_3$, belongs to the big family of compounds of the type $(CH_3)_4NMX_3$ with the bivalent metals M = Mn, Ni, Cd, Cu, or V and the halogen atoms X = Cl or Br [1]. Crystals of this family containing transition metals are extensively studied [1–12] because of their quasi-one-dimensional magnetic behaviour [2]. A quasi-one-dimensional behaviour (e.g. for the lattice heat capacity [3]) was also found for the diamagnetic crystal TMCC having infinite linear chains of the type (–M–Cl_3–M–Cl_3–), which are separated by tetramethylammonium (TMA) cations. All these compounds undergo several phase transitions at decreasing temperatures. Two structural first order phase transitions at

0953-8984/01/051119+13$30.00

118 K and 104 K have been observed for TMCC [4–7]. In the high temperature phase the crystal TMCC possesses a hexagonal [8, 9] structure with the space group $P6_3/m$ and $Z = 2$ formula units per unit cell. The lattice parameters are $\boldsymbol{a} = \boldsymbol{b} = 9.126$ Å, $\boldsymbol{c} = 6.718$ Å and $\gamma = 120^\circ$ [6]. At the first phase transition at 118 K the structure changes to a monoclinic one (phase II) with the space group $P2_1/m$ ($Z = 2$) and the lattice parameters $\boldsymbol{a} = 9.334$ Å, $\boldsymbol{b} = 8.796$ Å, $\boldsymbol{c} = 6.688$ Å with the monoclinic angle of $\gamma = 120.958^\circ$. For phase III below 104 K a space group $P2_1/b$ with $Z = 12$ formula units was determined. Here the lattice parameters are $\boldsymbol{a} = 8.84$ Å, $\boldsymbol{b} = 18.41$ Å, $\boldsymbol{c} = 20.0$ Å and $\gamma = 121.0^\circ$.

The TMA ($[(CH_3)_4N]^+$) cations are supposed to play a great role in the structural phase transitions. The mechanism of the phase transitions of TMCC is regarded to be of order–disorder type [10, 11] related to the ordering of TMA cations coupled to the displacive contributions originating from rotations of the MCl_3 chains, which are not yet understood in detail. The orientational disorder of the TMA groups is commonly described by the Frenkel model where the molecules jump between equally probable orientations. An important question in this context is the crystal structure in the phases at lower temperatures and the appearance of ferroelastic domains. In a recent paper the structural peculiarities of TMCC at lower temperatures were studied by means of quadrupolar perturbed ^{35}Cl NMR spectroscopy [12] and recently also by XRD diffraction measurements [6]. The main problem in the interpretation of the ^{35}Cl NMR measurements was the more complicated line splitting that cannot be understood by using the 'classical' group theoretical rule (see, e.g., Salje [13]) according to which the formation of three monoclinic domains is expected at the transition from the hexagonal into the monoclinic phase. As will be explained in section 3, the formation of domains can most obviously be seen in the ^{35}Cl NMR spectra if the crystals are rotated around the hexagonal axis $\boldsymbol{c}$ (in phase I). In the high temperature phase the 120° symmetry appears in the angular dependence of the ^{35}Cl NMR lines due to the threefold symmetry along the $CdCl_3$ chains. Below the phase transition at 118 K the ^{35}Cl NMR spectra reveal that the hexagonal structure is lost. The projections of the Cd–Cl bond directions upon the crystallographic $\boldsymbol{a}$, $\boldsymbol{b}$ plane differ now with respect to that in phase I by several degrees. Together with the formation of 120° domains, a line tripling is expected. However, an additional splitting of all resonance lines in phase II (in the temperature range from 118 K to 104 K) appeared. Additional reflection reflexes were also found in the x-ray diffraction pattern, which cannot simply be explained by the appearance of three monoclinic 120° domains.

It is the aim of this analysis to understand the specifics of the domain formation reflected both in the NMR and the XRD data, which seems not only to be a particular specific feature of TMCC but a problem which is present in many other compounds. For this reason it is necessary to check first to what extent the additional lines in the ^{35}Cl NMR spectra are due to the presence of chemically non-equivalent chlorine sites in the phases II and III or due to domains. In order to control the appearance of chemically non-equivalent chlorine sites ^{35}Cl NQR spectra are measured (section 3.1) which are independent of orientational influences. The ^{35}Cl NQR spectra are expected in the frequency range between 6 and 7 MHz according to the EFG tensors determined in the previous ^{35}Cl NMR studies [12]. In combination with the angular dependent ^{35}Cl NMR spectra it should then be possible to explain also the more complicated unit cells in the low temperature phase (section 3.2). The analysis of the domain formation seen in the ^{35}Cl NMR data will be based first on the symmetry analysis discussed in the papers by Aizu [14] and by Boulesteix [15] and then the epitaxial growth is discussed (section 4.1). In order to achieve a quantitative interpretation of the structural deformations, the elastic strains are calculated on the basis of a paper by Shuvalov *et al* [16] (section 4.2). Finally, the complete agreement between the

Table 1. ^{35}Cl NQR resonance frequencies ν_q (in MHz) for the different phases, measured at the temperatures T (in K) as indicated.

Phase	T	^{35}Cl NQR								
I	296				6.81					
I	120				6.85					
II	115			7.54	7.03	6.61				
III	95	7.61	7.38	7.36	7.05	6.99	6.92	6.84	6.74	6.61

results of NMR measurements and the x-ray diffraction pattern will be discussed (section 5), which shows that NMR spectroscopy enables a very detailed conclusion about the domain formation.

2. Experiment

For the experiments the same TMCC crystals were used as in our previous paper, which were grown at a temperature of 305 K by means of the slow evaporation method. The TMCC single crystal used in the NMR studies had a size of $3 \times 3 \times 4$ mm^3. The ^{35}Cl NMR measurements were performed at a magnetic field of $B_0 = 11.7$ T corresponding to a resonance frequency of 48.99 MHz, using an MSL500 NMR spectrometer (Bruker Analytic GmbH, Karlsruhe). Only the central transitions were measured. In order to reduce the influence of the dead time, a quadrupole echo sequence was taken with a 90° pulse width of 4 μs and a repetition time of 500 ms. The temperature variation close to the phase transitions was achieved in steps of 0.14 K. The real sample temperature was both controlled by the well known phase transition temperatures and by an additional calibration curve.

^{35}Cl nuclear quadrupole resonance (NQR) measurements were run on powdered TMCC samples of the same origin as the single crystal. The substance was filled into cylindrical glass tubes with a diameter of 10 mm. The NQR frequencies varied in a range between 6.6 MHz and 7.6 MHz at temperatures from 300 K to 95 K for which a special probe head was built up.

3. Results

3.1. ^{35}Cl NQR measurements for phase II

By means of ^{35}Cl NQR measurements, the number of chemically non-equivalent chlorine atoms can be determined in the different phases. The resonance frequencies measured are collected in table 1 and typical spectra are shown in figure 1. In order to ensure a good excitation of the various NQR lines shown in this figure, different offset frequencies had to be applied, which is not revealed here in detail. In complete agreement with the previous results of ^{35}Cl NMR measurements [12] and the hexagonal crystal structure, a single line appears at high temperatures (figure 1(a)). In the intermediate ferroelastic phase II three NQR lines are detected (figure 1(b)). This is consistent with the loss of the hexagonal symmetry in the ferroelastic phase and the presence of three chemically non-equivalent chlorine atomic sites per unit cell. In the phase III below 104 K (figure 1(c)) nine NQR lines with roughly equal intensities are detected. This clearly shows an increase of the size of the unit cell (at least a tripling), which will be discussed later in detail in comparison with x-ray diffraction measurements.

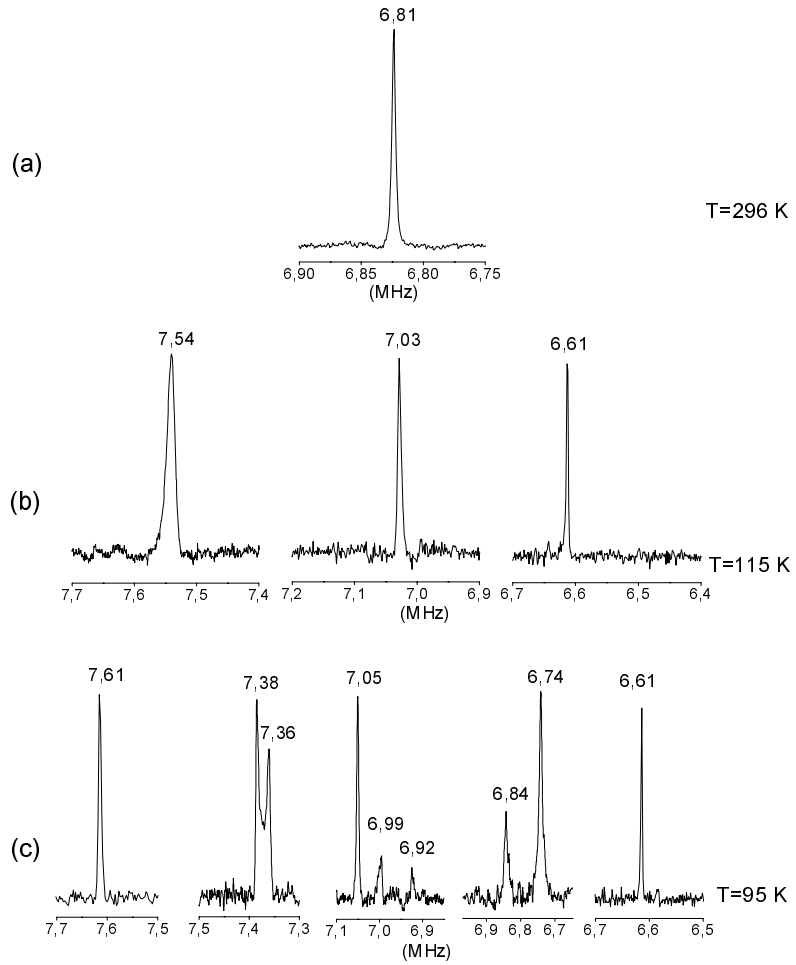

Figure 1. Typical ^{35}Cl NQR spectra of a polycrystalline TMCC sample in the different phases. (a) In the hexagonal phase at room temperature. (b) In the intermediate phase II at $T = 115$ K. (c) In the low temperature phase III at $T = 95$ K. All frequency values are given in MHz.

In the case of ^{35}Cl nuclei (with the spin quantum number $I = 3/2$) the NQR frequency ν_q is given by the expression [17, 18]:

$$\nu_q = \frac{e^2 Qq}{2h}\left(\sqrt{1+\frac{\eta^2}{3}}\right). \tag{1}$$

The interaction energy between the electric quadrupole momentum eQ of the nucleus and the electric field gradient eq can be described by the two parameters e^2Qq/h and η. The quantity e^2Qq/h is the quadrupole coupling constant (QCC). Q has the dimension of an area and is of the order of 10^{-24} cm^2, e is the elementary charge. The asymmetry parameter $\eta = (V_{XX} - V_{YY})/V_{ZZ}$ is defined by the components of the electric field gradient (EFG) tensor in the principal axis system (X, Y, Z).

The NQR frequencies ν_q in table 1 are in complete agreement with the values for η and $e^2Qq/(2h) = V_{ZZ}/2$ found by in the NMR measurements (table 2).

Table 2. Values of the EFG tensor elements V_{ZZ} (in units of MHz) in the principal axis system and the symmetry parameter η for the different phases, derived from the ^{35}Cl NMR measurements at the temperatures T (in K) as indicated.

Phase	T	$V_{ZZ}/2$									
I	296				6.74 $\eta = 0.16$						
I	120				6.82 $\eta = 0.13$						
II	115			7.49 $\eta = 0.12$	7.01 $\eta = 0.22$	6.32 $\eta = 0.27$					
III	98	7.59	7.36	7.34	6.99	6.95	6.93	6.76	6.65	6.52	

3.2. ^{35}Cl NMR measurements in phase II

Because of the relatively large quadrupole coupling constants, in the ^{35}Cl NMR measurements only the central transitions are considered, the line positions of which are determined by second order quadrupole effects. The EFG tensors were determined from the rotation patterns of the central transition frequencies which were measured for crystal rotations about the crystallographic $\boldsymbol{c}$ and $\boldsymbol{a}$ axes (in phase I). The well known Volkoff [18] formulae were applied, according to which the frequencies measured for the various rotation angles θ depend on the squares of the EFG tensor elements V_{ij}, with $i, j \in \{x, y, z\}$ in the laboratory frame with the z axis parallel to B_0. Furthermore, for phase II an orthogonal crystallographic frame $\boldsymbol{a}$, $\boldsymbol{b}^*$, $\boldsymbol{c}$ is defined, where the axis $\boldsymbol{b}^*$ is perpendicular to the crystallographic axes $\boldsymbol{c}$ and $\boldsymbol{a}$, where the directions of the latter are the same as in phase I. For a rotation around the crystallographic axis $\boldsymbol{a}$ (rotational angle θ_a), the second order shift $\Delta\nu$ of a central ^{35}Cl NMR line is given by the following formulae, where ν_L is the Larmor frequency:

$$\begin{aligned}
\Delta\nu(\theta_a) &= \frac{1}{\nu_L}[n_a + p_a\cos(2\theta_a) + r_a\sin(2\theta_a) + u_a\cos(4\theta_a) + v_a\sin(4\theta_a)] \\
n_a &= \frac{1}{192}\left\{9V_{xx}^2 - 14\left[\frac{1}{4}(V_{yy} - V_{zz})^2 + V_{yz}^2\right] - 8(V_{xz}^2 + V_{xy}^2)\right\} \\
p_a &\frac{1}{32}[V_{xx}(V_{yy} - V_{zz}) + 4(V_{xz}^2 - V_{xy}^2)] \\
r_a &= \frac{1}{16}[-V_{xx}V_{yz} + 4V_{xz}V_{xy}] \\
u_a &= \frac{3}{32}\left[\frac{1}{4}(V_{yy} - V_{zz})^2 - V_{yz}^2\right] \\
v_a &= \frac{3}{32}(V_{zz} - V_{yy})V_{yz}.
\end{aligned} \tag{2}$$

The analysis of these measurements has been described in detail in our previous paper [12]. We have determined the complete electric field gradient tensors of the ^{35}Cl nuclei both in the paraelectric high temperature phase I (above 118 K) and in the ferroelastic phase II. The principal values V_{ZZ} of the tensors (in units of MHz), the asymmetry values η and the directions of the principal axes of the tensors are summarized in table 2. On this basis it could be shown at first that the phase transition from the high temperature phase with hexagonal symmetry ($P6_3/m$ above 118 K) to the monoclinic one ($P2_1/m$) is clearly visible in the ^{35}Cl NMR spectra. The phase transition is accompanied by the appearance of three chemically non-

equivalent Cl sites in the unit cell in complete agreement with the NQR results as reported above.

Because the influence of the reduced symmetry on the ^{35}Cl NMR spectra is now clarified, the influence of the domain structure can be deduced from the spectra. Because the $\boldsymbol{c}$ axis is the former sixfold screw axis, the now formed domain lattices merge by rotations around this axis. Therefore, the structural changes related to this domain formation may directly be derived from the NMR rotation pattern around the $\boldsymbol{c}$ axis which has already been measured in the previous paper [19]. In connection with the results from the NQR measurements presented above it becomes now completely clear that the splitting of each of the resonance lines into two components is related with the appearance of orientational twins. Instead of the usual monoclinic 120° domains, pairs of twin domains do occur differing in their orientations by an angle of about 4°.

However, the domain formation shows also defined implications for other crystal orientations which can be used to examine the expected behaviour. Hence, NMR measurements were carried out here for orientations where the crystallographic $\boldsymbol{a}$ axis is oriented approximately parallel to the rotation axis. Typical spectra are shown in figures 2(a) and 2(b). As known from the XRD data, one of the Cd-Cl directions is almost parallel to the $\boldsymbol{a}$ axis in phase I. Therefore, the $\boldsymbol{a}$-rotation pattern in phase I shown in figure 3(a) can be easily interpreted. Because of the almost axial quadruple tensor of the three chemically equivalent Cl nuclei, the line with the weak angular dependence belongs to those Cl atoms whose Cl–Cd bond directions are almost in parallel to $\boldsymbol{a}$, whereas the two other lines exhibiting strong positional changes are due to the other two types of Cl nucleus. In the monoclinic phase II, the Cl positions become chemically non-equivalent, but their bond directions only change by a few degrees. However, six ^{35}Cl NMR lines (denoted by K1, K2, L1, L2, M1 and M2 in figure 3(b) can now be distinguished with the weak angular dependence as typical for a Cl nucleus with its Cd–Cl bond direction almost parallel to the rotation axis. Since we know from the ^{35}Cl NQR measurements presented here that there are only three chemically different Cl sites, the additional lines must result from the domain formation. This situation may be explained in a rather simple way. In the case of a single domain monoclinic crystal, only one ^{35}Cl NMR line is to be expected, showing weak angular dependence. But in a crystal with 120° domains, in the other two domains each one of the other two chemically non-equivalent Cl positions is rotated around the common $\boldsymbol{c}$ axis of the domains in such a manner that its Cd–Cl bond direction almost coincides with the rotation axis. This situation may explain a line tripling. But there is an additional pair splitting of each of the three lines. As will be shown in section 4, a more complicated domain structure is conceivable from symmetry and crystallographic considerations showing rotational twin domains with a rotation angle of 4°, which explains this splitting into the six experimentally observed lines.

3.3. NMR measurements in phase III

The NMR measurements in phase III can directly be analysed in comparison with the available x-ray data. Only those ^{35}Cl NMR measurements will be discussed in which the crystallographic $\boldsymbol{a}$ axis of phase I is aligned approximately parallel to the rotation axis. In this special orientation the total number of lines can most precisely be analysed. The result of the measurement is shown in figure 3(c). The increase of the total number of resonance lines by a factor of three can be clearly seen if one compares the ^{35}Cl NMR spectrum for this special orientation in figure 4(a) in phase I at 123 K and figure 4(b) in phase II at 113 K with the analogous spectrum in figure 4(c) (in phase III at 98 K), where 18 lines are present. The drastic increase of the number of lines in the spectra occurs directly at the phase transition. This finding has been

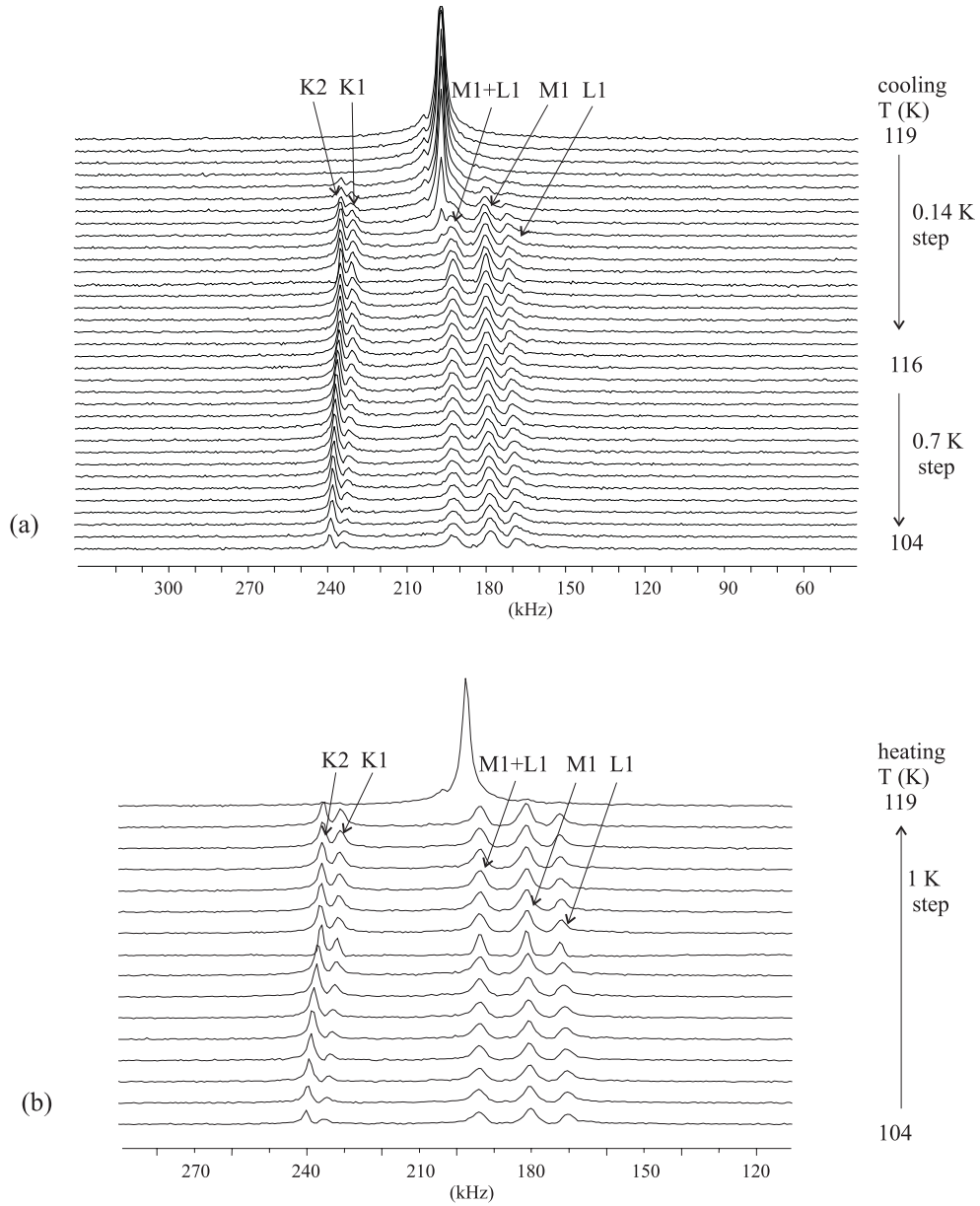

Figure 2. Temperature dependence of the ^{35}Cl NMR spectra of TMCC on cooling (a) and heating (b). For this measurement the axis $\boldsymbol{a}$ is perpendicular to the magnetic field and the axis $\boldsymbol{c}$ inclines at an angle of $\theta_a \approx 120^\circ$ with the magnetic field.

checked by repeated measurements with changing the temperatures both from lower (starting in the phase below 104 K) to higher temperatures and *vice versa* (beginning from temperatures above 118 K). First of all it could be clearly seen that there is no structurally incommensurate modulation of the lattice parameters leading to an increasing broad distribution of resonance frequencies with increasing temperature difference from the phase transition. Moreover, it

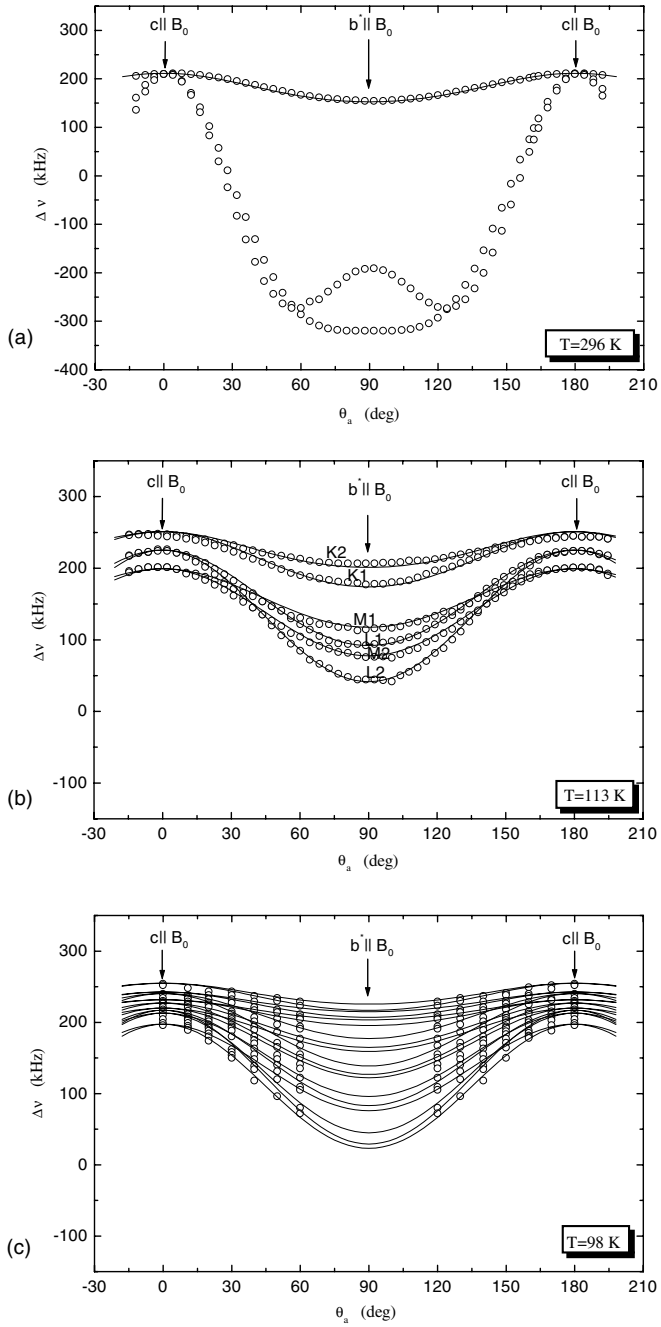

Figure 3. Angular dependence of the ^{35}Cl NMR central lines of TMCC (denotation see text), when the crystal is rotated about the $\boldsymbol{a}$ axis perpendicular to the magnetic field (so called selective orientation). (a) In the hexagonal phase I at room temperature. (b) In the intermediate phase II at 113 K. The six lines (K1, K2, L1, L2, M1, M2) in phase II for the ^{35}Cl nuclei in the orientation of one principal axis of the EFG tensors in the vicinity to the crystallographic $\boldsymbol{a}$ axis reflect the orientation of the ferroelastic domains. (c) In the low temperature phase III at $T = 98$ K. The circles in the rotation patterns represent the experimental data, the full curves are calculated according to equations (2).

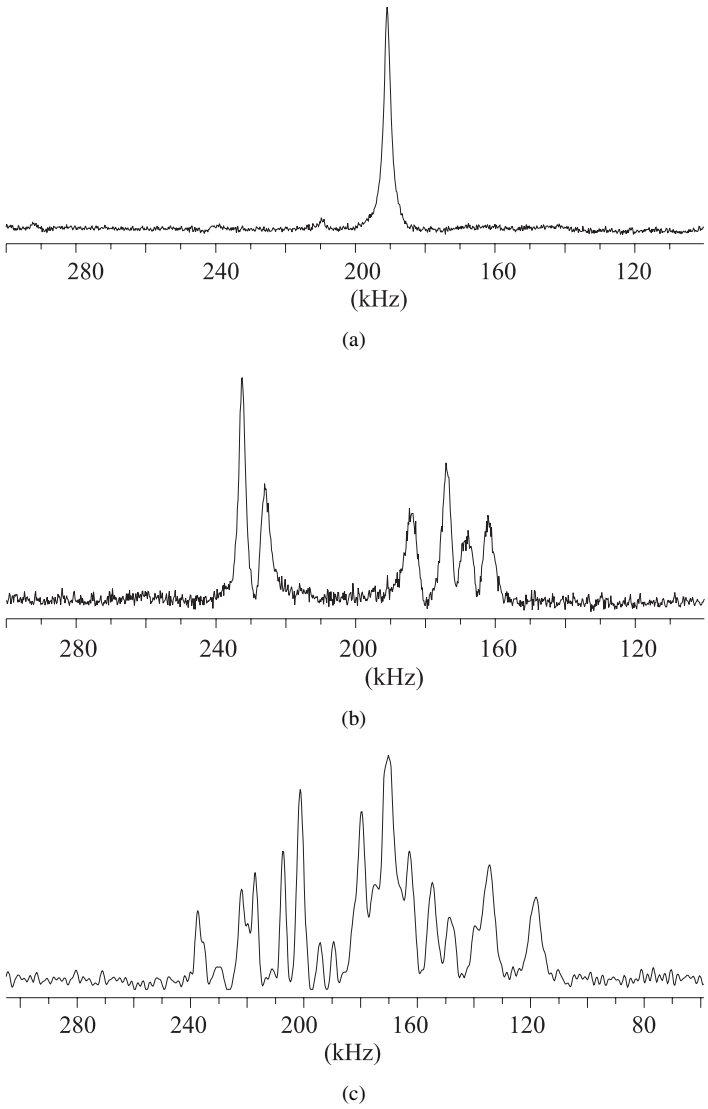

Figure 4. (a) NMR spectra in phase I at 123 K, (b) in phase II at 113 K and (c) in phase III at 98 K, which show the increase of the number of lines due to the enlarged unit cell. The orientation is chosen in the following way: the $\boldsymbol{a}$ axis is perpendicular to $\boldsymbol{B}_0$ and the $\boldsymbol{c}$ axis inclines at an angle of $\theta_a = 45^\circ$ with $\boldsymbol{B}_0$, $\theta_a = \angle(\boldsymbol{c}, \boldsymbol{B}_0)$.

can be shown that the relative intensity of all lines does not change if the measurements are started at low or at high temperatures. Since there is no doubt that the unit cell contains $Z = 12$ formula units below 104 K the increased number of lines (factor of three in the NMR studies as compared with the intermediate phase and the same factor as found in the NQR measurements) can be well understood if the existence of the domains already discussed is further assumed and if now nine different chlorine atoms are present in a unit cell. This exactly confirms the x-ray data for phase III.

4. Discussion

4.1. Interpretation of ferroelastic domain structure in phase II. Analysis of symmetry

In the paper of Aizu [14] the formation of three monoclinic (120°) domains is explained by the loss of the sixfold symmetry axis at the transition from the hexagonal room temperature phase I with space group $P6_3/m$ into the monoclinic phase II with space group $P2_1/m$. Within this approach (based exclusively on symmetry arguments) the formation of a more complicated ferroelastic domain structure can only be understood by an additional loss of symmetry operations [13, 14] at the phase transition as described, for instance, in the papers of Boulesteix [15]. According to [15], the number of orientation domains is equal to the ratio n_{01} of the order of the point group g_0 of the high-symmetry structure S_0 to the order of the intersection $g_0 \cap g_1$ of g_0 and g_1 with g_1 being the point group of the low symmetry structure S_1, i.e.

$$n_{01} = \frac{\text{order of } g_0}{\text{order of } g_0 \cap g_1}. \tag{3}$$

S_0 is hexagonal ($P6_3/m$) with $g_0 = 12$ symmetry operations:

(1) x, y, z	(2) $\bar{y}, x-y, z$	(3) $\bar{x}+y, \bar{x}, z$
(4) $\bar{x}, \bar{y}, z+\frac{1}{2}$	(5) $y, \bar{x}+y, z+\frac{1}{2}$	(6) $x-y, x, z+\frac{1}{2}$
(7) $\bar{x}, \bar{y}, \bar{z}$	(8) $y, \bar{x}+y, \bar{z}$	(9) $x-y, x, \bar{z}$
(10) $x, y, \bar{z}+\frac{1}{2}$	(11) $\bar{y}, x-y, \bar{z}+\frac{1}{2}$	(12) $\bar{x}+y, \bar{x}, \bar{z}+\frac{1}{2}$.

S_1 is monoclinic $P2_1/m$ with $g_1 = 4$ symmetry operations:

(1) x, y, z (2) $\bar{x}, \bar{y}, z+\frac{1}{2}$ (3) $\bar{x}, \bar{y}, \bar{z}$ (4) $x, y, \bar{z}+\frac{1}{2}$.

If the symmetry elements of the low symmetry structure S_1 are parallel to their homologues in the high symmetry structure S_0, the Aizu [14] result

$$n_{01} = \frac{\text{order of } g_0}{\text{order of } g_1} \tag{4}$$

is correct because $g_0 \cap g_1 = g_1$. However, if the low symmetry phase grows epitaxially on the high symmetry structure, the real domains show small disorientations from the 120° arrangement due to the deviation of the monoclinic angle from 120° (being reflected by the appearance of three non-equivalent chlorine atoms per unit cell as shown above). Consequently, the symmetry elements of S_0 and S_1 are no longer parallel and $g_0 \cap g_1$ is the point group 1 unless both structures are centrosymmetric. In this case, the inversion symmetry remains and the order of the intersection $g_0 \cap g_1$ is equal to 2. Therefore, the number of expected domains results as

$$n_{01} = \frac{\text{order of } g_0}{2}. \tag{5}$$

Since for the hexagonal high symmetry structure S_0 the order of g_0 is 12, we expect six different domains. However, although this number coincides with the observed number of domains in the NMR measurements the above explanation has some drawbacks inasmuch the number of domains detected by x-ray diffraction is higher (12). The important point in these x-ray diffraction data is, however, that only reflections are found which are displaced by angles of 4°, 8° or 12°. This again shows the 'misorientation' as found in the ^{35}Cl NMR measurements. A more quantitative explanation of the domain structure can be obtained using the approach of Shuvalov *et al* [16]. The formation of additional twin domains is understandable as a growing of twins from twin domains resulting in angles of multiples of 4°.

4.2. Orientation of domains

Whereas from the classical point of view three equivalent monoclinic 120° orientation domains would be expected for a $6_3/mF2_1/m$ ferroelastic transition, six or 12 equivalent orientation domains really occur with the relative angles $+\Theta/2$, $-\Theta/2$, $120^\circ + \Theta/2$, $120^\circ - \Theta/2$, $240^\circ + \Theta/2$, $240^\circ - \Theta/2$, $+\Theta$, $-\Theta$, $120^\circ + \Theta$, $120^\circ - \Theta$, $240^\circ + \Theta$, $240^\circ - \Theta$ between their structural orientation in the plane perpendicular to the monoclinic axis c.

To derive the relative domain orientations quantitatively we evaluate the spontaneous strain tensor components according to [16]. By means of this approach the saturated angle Θ_s can be calculated from the strain tensors of the three Aizu orientation states e_{ij}^{S1}, e_{ij}^{S2}, e_{ij}^{S3} having the form [6]

$$
\begin{aligned}
e_{ij}^{S1} &= \begin{pmatrix} -u & v & 0 \\ v & u & 0 \\ 0 & 0 & 0 \end{pmatrix} \\
e_{ij}^{S2} &= \begin{pmatrix} -(u/2 + v\sqrt{3}/2) & -v/2 - u\sqrt{3}/2 & 0 \\ -v/2 - u\sqrt{3}/2 & -u/2 + v\sqrt{3}/2 & 0 \\ 0 & 0 & 0 \end{pmatrix} \\
e_{ij}^{S3} &= \begin{pmatrix} -(u/2 - v\sqrt{3}/2) & -v/2 + u\sqrt{3}/2 & 0 \\ -v/2 + u\sqrt{3}/2 & -u/2 - v\sqrt{3}/2 & 0 \\ 0 & 0 & 0 \end{pmatrix}
\end{aligned} \tag{6}
$$

with $u = (e_{11} - e_{22})/2$, $v = e_{12}$, and the spontaneous strain components [13].

$$
\begin{aligned}
e_{11} &= \frac{a \sin\gamma}{a_0 \sin 120^\circ} - 1 \\
e_{22} &= \frac{b}{a_0} - 1 \\
e_{12} &= \frac{1}{2} \frac{a \cos\gamma - b \cos 120^\circ}{a_0 \sin 120^\circ}.
\end{aligned} \tag{7}
$$

a, b and γ are the relevant cell parameters in phase II. The condition that the strain tensor components vanish in the average structure, i.e. in the hexagonal structure to phase II, leads to the equation [6]

$$
(e_{11} + e_{22})/2 = \frac{1}{2}\left(\frac{a \sin\gamma}{a_0 \sin 120^\circ} + \frac{b}{a_0} - 2\right) = 0.
$$

Hence, the cell parameter a_0 extrapolated from phase I into phase II, follows from the equation

$$
a_0 = \frac{a \sin\gamma + b \sin 120^\circ}{2 \sin 120^\circ}
$$

and can be directly calculated from the lattice parameters a, b and γ in phase II.

The saturated rotational angle between the epitaxially grown domains is given by [16] $\Theta_s = \sqrt{3(u^2 + v^2)}$ and results in phase II in a theoretical value $\Theta_s = 3.5^\circ$ in good agreement with the experimentally observed rotation angle $\Theta_{\text{exp}} = 4^\circ$ of the EFG tensors and the XRD reflections. The correspondence is well enough to confirm our explanation also quantitatively.

The authors of [16] note also that orientational domains may exist with rotational angles $0^\circ, \pm\Theta, \pm 2\Theta$ and with different proportions of the total volume, depending on the macroscopic shape of the domain configurations (i.e. spiral shaped, starlike or double starlike shaped).

5. Conclusions

The presented ^{35}Cl NMR and ^{35}Cl NQR results make evident that the structural peculiarities found in the recent XRD studies by [6] are neither due to an incommensurately modulated

structure nor to an enlarged unit cell size in the phase II (between 118 and 104 K) but due to the peculiarities of the ferroelastic domain structure. The measurements reveal that the TMCC crystal shows a more complicated domain structure as the result of the epitaxial growth of rotational twin domains [20]. The enhancement in the number of domains is provoked to diminish stresses in the domain walls [21]. Distortion angles of about 4 degrees with respect to the normal 120 degree domains are directly derived from the NMR data. The distortion angle between the rotational twins calculated by means of the strain tensors is in quantitative agreement with the experiment. The suggested interpretation of the NMR spectra in the intermediate phase II is also confirmed by the number of NMR lines in the low temperature phase III in agreement with the symmetry change $P2_1/m$ $(Z = 2) \rightarrow P2_1/b$ $(Z = 12)$.

The more complicated domain structure finds its expression also in the XRD measurements. The authors of [6] revealed a number of additional reflections of different intensities, which have been interpreted by the supposition of four different sub-lattices (A, B, C, D). These sub-lattices arise by rotations around the crystallographic $\boldsymbol{c}$ axis by angles of multiples of $\sim 4^\circ$, similarly as derived from the NMR results. Furthermore, in the XRD measurements two out of the four sub-lattices reveal only fairly weak reflections. Probably, also limitations in sensitivity in the NMR measurements may be the reason which they show up only the spectra of those six domains owning the largest volume.

The remaining question in this context is the role of the TMA ions during the phase transitions. From our measurements and also from the x-ray studies it became evident that the lattice and symmetry changes of the three phases can be monitored by the chlorine atoms. Although each symmetry reduction should imply some reconfiguration of the TMA ions, changes in the TMA degrees of order have still not been analysed. For this reason, further NMR measurements on the ^{14}N nuclei of the TMA ions are in progress.

Acknowledgments

The authors gratefully acknowledge the financial support by the Deutsche Forschungsgemeinschaft (DFG), the "Axel Springer Stiftung", the Deutscher Akademischer Austauschdienst (DAAD) and the University of the Basque Country (UPV project EB098/97). They are indebted to Professor Z Czapla (Wroclaw, Poland) for growing the crystals and for valuable comments. One of us (IP) is indebted to the Basque Government for financial support.

References

[1] Gesi K 1992 *Ferroelectrics* **137** 209
[2] Dingle R, Lines M E and Holt S L 1969 *Phys. Rev.* **187** 643
[3] Kopinga K, van der Leeden P and de Jonge W J M 1976 *Phys. Rev.* B **14** 1519
[4] Tsang T and Utton D B 1976 *J. Chem. Phys.* **64** 3780
[5] Braud M N, Couzi M, Chanh N B, Courseille C, Gallois B, Hauw C and Mersse A 1990 *J. Phys.: Condens. Matter* **2** 8209
[6] Peral I, Madariaga G, Perez-Etxebarria A and Breczewski T 2000 *Acta Crystallogr.* B **56** 215
[7] Díaz-Hernández J, Aguirre-Zamalloa G, López-Echarri A, Ruiz-Larrea I, Breczewski T and Tello M J 1997 *J. Phys.: Condens. Matter* **9** 3399
[8] Morosin B 1972 *Acta Crystallogr.* B **28** 2303
[9] Peercy P S, Morosin B and Samara G A 1973 *Phys. Rev.* B **8** 3378
[10] Jewess M 1982 *Acta Crystallogr.* B **38** 1418
[11] Couzi M and Mlik Y 1986 *Raman Spectrosc.* **17** 117
[12] Mulla-Osman S, Michel D, Czapla Z and Hoffmann W-D 1998 *J. Phys.: Condens. Matter* **10** 2465
[13] Salje E K H 1990 *Phase Transitions in Ferroelastic and Co-elastic Crystals* (Cambridge: Cambridge University Press)

[14] Aizu K 1970 *J. Phys. Soc. Japan* **28** 706
[15] Boulesteix C 1984 *Phys. Status Solidi* a **86** 11
[16] Shuvalov A L, Dudnik E F and Wagin S V 1985 *Ferroelectrics* **65** 143
[17] Krüger H 1951 *Z. Phys.* **130** 371
[18] Volkoff G M 1953 *Can. J. Phys.* **31** 820
[19] Mulla-Osman S, Michel D, Völkel G and Czapla Z 2000 *Phys. Status Solidi* b **219** 9
[20] Hahn T, Janovec V and Klapper H 1999 *Ferroelectrics* **222** 11
[21] Sapriel J 1975 *Phys. Rev.* B **12** 5128